10606 *Biochemistry* **2010,** *49,* 10606–10615
DOI: 10.1021/bi100927p

BIOCHEMISTRY
including biophysical chemistry & molecular biology
Article

An Investigation of the Distal Histidyl Hydrogen Bonds in Oxyhemoglobin: Effects of Temperature, pH, and Inositol Hexaphosphate[†]

Yue Yuan, Virgil Simplaceanu, Nancy T. Ho, and Chien Ho*

Department of Biological Sciences, Carnegie Mellon University, Pittsburgh, Pennsylvania 15213, United States

Received June 9, 2010; Revised Manuscript Received November 12, 2010

ABSTRACT: On the basis of X-ray crystal structures and electron paramagnetic resonance (EPR) measurements, it has been inferred that the O_2 binding to hemoglobin is stabilized by the hydrogen bonds between the oxygen ligands and the distal histidines. Our previous study by multinuclear nuclear magnetic resonance (NMR) spectroscopy has provided the first direct evidence of such H-bonds in human normal adult oxyhemoglobin (HbO_2 A) in solution. Here, the NMR spectra of uniformly ^{15}N-labeled recombinant human Hb A (rHb A) and five mutant rHbs in the oxy form have been studied under various experimental conditions of pH and temperature and also in the presence of an organic phosphate, inositol hexaphosphate (IHP). We have found significant effects of pH and temperature on the strength of the H-bond markers, i.e., the cross-peaks for the side chains of the two distal histidyl residues, α58His and β63His, which form H-bonds with the O_2 ligands. At lower pH and/or higher temperature, the side chains of the distal histidines appear to be more mobile, and the exchange with water molecules in the distal heme pockets is faster. These changes in the stability of the H-bonds with pH and temperature are consistent with the changes in the O_2 affinity of Hb as a function of pH and temperature and are clearly illustrated by our NMR experiments. Our NMR results have also confirmed that this H-bond in the β-chain is weaker than that in the α-chain and is more sensitive to changes in pH and temperature. IHP has only a minor effect on these H-bond markers compared to the effects of pH and temperature. These H-bonds are sensitive to mutations in the distal heme pockets but not affected directly by the mutations in the quaternary interfaces, i.e., $\alpha_1\beta_1$ and/or $\alpha_1\beta_2$ subunit interface. These findings provide new insights regarding the roles of temperature, hydrogen ion, and organic phosphate in modulating the structure and function of hemoglobin in solution.

Hemoglobin (Hb) is a tetrameric, heme-containing protein consisting of two α- and two β-chains and is the carrier of oxygen from lungs to tissues in vertebrates. Oxygen binding to Hb is reversible and cooperative (*1*). The ratio of the equilibrium-binding constants for CO and O_2 is approximately 20000 for free heme and is lowered to about 250 in the case of Hb A[1] (*2*). Thus, the relative affinity for O_2 versus CO is greatly increased in Hb, due to having its hemes embedded in the heme pockets of the protein molecule and interacting with their environment. It is currently accepted that O_2 bound to Hb is stabilized by the hydrogen bonds between oxygen ligands and the distal histidyl residues. Early X-ray crystal structural studies at moderate resolution of 2.1 Å (*3*) suggested the existence of a H-bond in the α-heme pocket between the bound oxygen and the distal histidine E7 (αHis58) and possibly a very weak one in the β-heme pocket to the E7 (βHis63) histidine. High-resolution (1.25 Å) X-ray crystal structures (*4*) gave further support to this idea. The existence of such an H-bond has been inferred from the crystal structures (*4*) to explain the stronger binding of O_2 to Hb and Mb, relative to the free heme. Although reasonable, this suggestion has remained controversial due to a lack of direct experimental evidence, especially for Hb in solution, under physiological conditions (*5*−*8*). Our previous NMR study (*9*) has provided the first direct evidence for the presence of the distal histidyl H-bonds in HbO_2 A in solution. Here, we investigate the stability of these H-bonds as affected by pH, temperature, and an organic phosphate, inositol hexaphosphate (IHP). We have also examined the change to these H-bonds caused by mutations at the subunit interfaces ($\alpha_1\beta_1$ and $\alpha_1\beta_2$) and at the distal heme pockets. Uniformly ^{15}N-labeled recombinant human normal adult hemoglobin A (rHb A) and five recombinant mutant rHbs were prepared, and the NMR spectra were recorded on Bruker AVANCE DRX-600 MHz spectrometers. The changes in the stability of the H-bonds with pH and temperature are consistent with the changes in the affinity of Hb for O_2 and are clearly shown by our NMR experiments. We have found that the H-bond markers, namely, the cross-peaks for α58His ($^1H\varepsilon_2$, $^{15}N\varepsilon_2$) and β63His ($^1H\varepsilon_2$, $^{15}N\varepsilon_2$) are significantly affected by pH and temperature. At lower pH and/or higher temperature, the side chains of the distal histidines appear to be more mobile and the proton exchange with water molecules in the distal heme pocket is faster, causing these markers to lose intensity and even to disappear. Our present findings have confirmed that the H-bond in the β-chain is weaker than that in the α-chain as suggested by the crystallographic studies (*3*, *4*). The allosteric effector, inositol hexaphosphate (IHP), binds to Hb and decreases its affinity for O_2. However, the H-bond markers, the cross-peaks for α58His ($^1H\varepsilon_2$, $^{15}N\varepsilon_2$) and

[†]This work is supported by a research grant from the National Institutes of Health (R01GM084614).

*Address all correspondence to this author. Phone: 412-268-3395. Fax: 412-268-7083. E-mail: chienho@andrew.cmu.edu.

[1]Abbreviations: Hb A, human normal adult hemoglobin; rHb, recombinant Hb; HbO_2, oxyhemoglobin; HbCO, carbonmonoxyhemoglobin; deoxy-Hb, deoxyhemoglobin; met-Hb, methemoglobin; NMR, nuclear magnetic resonance; IHP, inositol hexaphosphate; HSQC, heteronuclear single-quantum coherence; HMQC, heteronuclear multiple quantum coherence.

 Published on Web 11/15/2010

β63His ($^1H\varepsilon_2$, $^{15}N\varepsilon_2$), do not change significantly upon the addition of IHP at pH 8.0 and 7.0, although these peaks become weaker, suggesting that the effect of IHP might not be strong enough to break these H-bonds under those conditions.

MATERIALS AND METHODS

Sample Preparation. Uniformly ^{15}N-labeled rHb A and five mutant rHbs, rHb (αV96W), rHb (αV96W/βN108K), rHb (βD99N), rHb (αY42D/βD99N), and rHb (αL29W), were expressed in *Escherichia coli* JM109 from the plasmids pHE2, pHE202, pHE249, pHE208, pHE222, and pHE285, respectively (*10*−*14*). rHbO_2 A samples for NMR experiments were prepared in phosphate-buffered solution (100 mM Na_2HPO_4/NaH_2PO_4, 10% D_2O) at pH 6.5, 7.0, and 8.0, respectively, using standard procedures in our laboratory (*15*). The final protein concentration was 0.7−1 mM (tetramer). The samples with IHP were prepared by adding IHP stock solution to the rHb samples to a final concentration of 5 mM. An important consideration in our NMR experiments was sample stability, especially at lower pH and higher temperatures, because the diamagnetic oxy-Hb can readily oxidize to the high-spin ferric, paramagnetic aquomet-Hb, where no heme-pocket resonances can be observed. The freshly prepared oxy-form rHb samples can usually stay in oxy form without met-Hb being detected for several hours, which gives us time to finish the NMR experiments at one experimental condition. Then, the samples are repurified according to the standard procedures in our laboratory and prepared carefully for the next experimental condition.

NMR Spectroscopy. NMR spectra were recorded on Bruker AVANCE DRX-600 MHz spectrometers. As the resonances of distal histidine side chains are essentially under the water resonance (*9*), the water suppression quality is of paramount importance, and no water-directed suppression technique (presaturation, excitation sculpting, selective excitation, or flip-back) can be employed, as they would also suppress the resonances of interest. Echo-antiecho gradient-selected HSQC experiments (hsqcetf3gp from the Bruker standard library) (*16*) had to be used so that only the signals from the protons attached to ^{15}N nuclei are refocused and detected, while the magnetization belonging to protons attached to any other nuclei (^{14}N, ^{12}C, ^{13}C, ^{16}O, etc.) remains scrambled and therefore gives no signal. No other water suppression technique was employed, and no postacquisition solvent-filtering software processing was used. A first set of experiments were carried out using a 5 mm TXI *z*-gradient CryoProbe. Unfortunately, the poor water suppression due to the radiation damping effects and other instrumental causes rendered the higher sensitivity of this probe useless in our case. The rest of the experiments were then carried out at 600 MHz, but with a conventional 5 mm TXI *xyz*-gradient probe, using magic-angle gradients, which gave satisfactory results. Typical spectral widths were 20 ppm (^1H) and 200 ppm (^{15}N) with carriers at 4.7 and 175 ppm, 2048 and 256 time-domain points, respectively. The refocusing delay in the INEPT module was 5.5 ms in order to select the signals from the ^1H directly attached to ^{15}N. With 16 or 32 scans per increment, 2D spectra were acquired typically in 2.5 or 5 h blocks. At lower temperatures, the INEPT delay was shortened to compensate for the signal loss due to the increased line widths.

RESULTS

Effect of pH. In our earlier paper (*9*), the HMQC spectra for HbO_2 A provided the first direct evidence for the existence of the distal histidyl H-bonds in HbO_2 A at 29 °C and pH 8.0. That condition was chosen to make use of the increased stability of the Hb molecule against autoxidation and also because the oxygen affinity is higher at this pH than at lower pH values. In our present study, the NMR experiments were carried out at three different pH values in the absence and presence of IHP, respectively. First, HSQC and HMQC experiments were carried out at pH 8.0 and 29 °C in 0.1 M phosphate in the absence of IHP as control. Two cross-peaks, which correspond to the H-bonds between the oxygen ligand and the side chains of α58 and β63 distal histidines in HbO_2 A, are shown clearly in the HSQC (Figure 1B) and in the HMQC spectra (result not shown). Then, HbO_2 A samples were prepared at pH 7.0 and 6.5, and the HSQC experiments were carried out at 29 °C. At pH 7.0 (Figure 1E), the cross-peak for α58His ($^1H\varepsilon_2$, $^{15}N\varepsilon_2$) is visible, indicating that the H-bond still exists at this pH. However, the cross-peak for β63His ($^1H\varepsilon_2$, $^{15}N\varepsilon_2$) disappears at pH 7.0. At pH 6.5 and 29 °C, the cross-peaks from α58 and β63 distal histidines cannot be observed (Figure 1G), suggesting that the H-bonds are broken at lower pH. To further illustrate the changes in the peak intensity of β63His under various experimental conditions, horizontal 1D slices along the ^1H axis through the cross-peak of β63His are taken from the 2D spectra of Figure 1 and shown in Figure 2. These 1D slices also demonstrate that using the technique described in the section on Materials and Methods, we are able to detect the cross-peaks of the H-bonded distal histidine side chains in oxyhemoglobin when they exist, regardless of their positions with respect to the resonance of water. The first column (A, D, and F) of Figures 1 and 2 shows the experimental data collected at 7 °C and pH 8.0, 7.0, and 6.5, respectively. At this low temperature, the peak of β63His is well resolved from the water signal, and it is strong at pH 8.0. The peak becomes weaker at pH 7.0 and then disappears at pH 6.5. This peak also shifts upfield slightly, away from the water, as pH is lowered. The residual water signal is practically midway between the α58His and the β63His peaks, so if there was an attenuation of these signals by the "suppression of the water signal", the α58His peak should have been diminished, too. That is not the case. We also collected data at 11 and 20 °C for each pH condition. When the temperature goes up, the water signal is shifting upfield (toward the right-hand side of the spectra) and is getting closer to the peak of β63His. At 11 °C and pH 8.0, the peak of β63His is clearly observed but is very weak at pH 7.0 and not seen at pH 6.5. At 20 °C and pH 8.0, the signals from water and β63His are very close. But, we are still able to recognize the signal of β63His since it is broad and the water signal is sharp. When the temperature is raised to 29 and 37 °C, the water signal already shifts to the right side of the signal from β63His (Figure 2B,C). At pH 8.0, the peak of β63His is observed at 29 °C and is getting weaker at 37 °C. In conclusion, the peak of β63His is observed at pH 8, and the peak intensities are getting weaker when the temperature changes from 7 to 37 °C. However, at pH 7.0, the peak of β63His can only be observed at 7 and 11 °C (Figure 2). The β-chain peak is visible when it exists and not visible when it does not. Our results clearly show a trend, namely, the peak is weaker in the β-chain distal heme pocket, and the distal histidine peaks in both α- and β-chains are weaker when the affinity of Hb for oxygen is lower.

Effect of Temperature. It is known that the temperature affects the oxygen binding to Hb (*17*). An increase in temperature decreases its affinity and thus enhances the release of oxygen. For example, at pH 6.5, the measurements show P_{50} values of 4.3 mmHg at 7 °C and 21.5 mmHg at 29 °C (Figure 3). The effect of

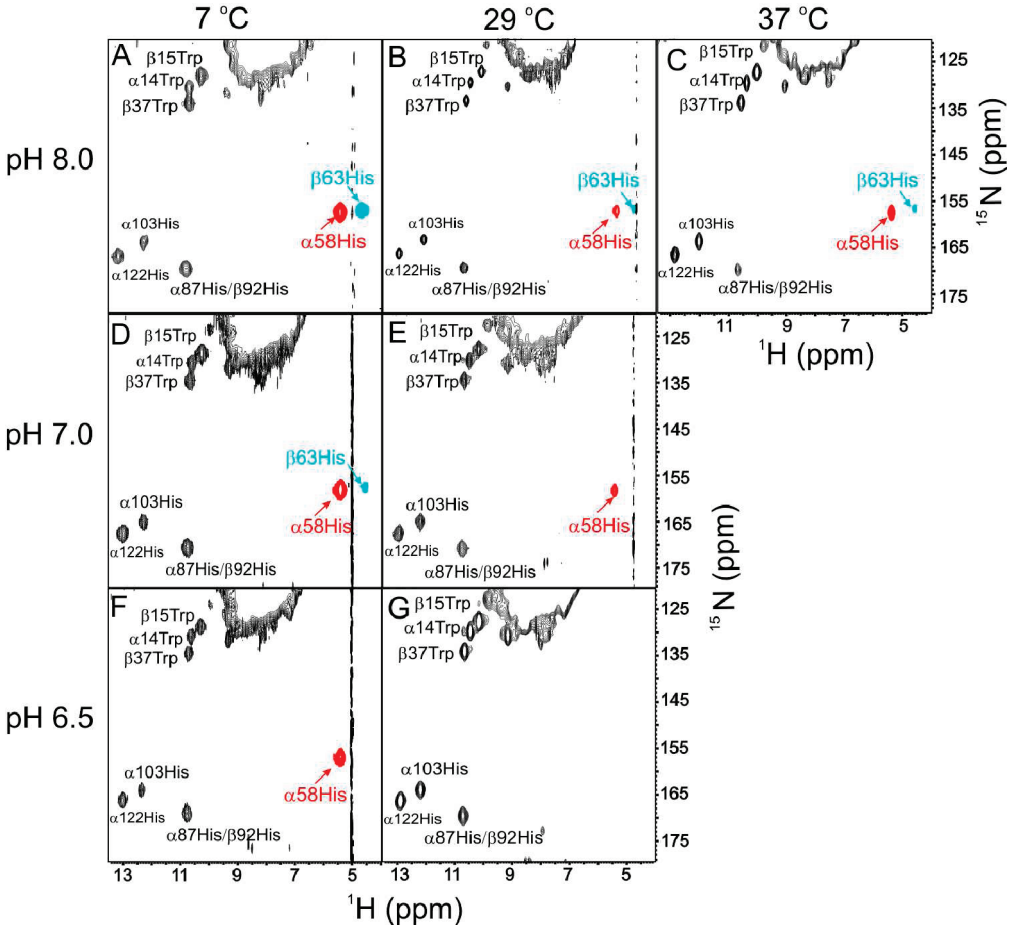

FIGURE 1: His and Trp side-chain regions of 600 MHz (^{1}H,^{15}N) HSQC spectra of fully ^{15}N-labeled HbO_2 A in H_2O at pH 8.0 (upper row), 7.0 (middle row), and 6.5 (lower row) at 7, 29, and 37 °C, respectively. The cross-peaks for the relevant directly bonded ^{15}N−^{1}H pairs are identified for each residue.

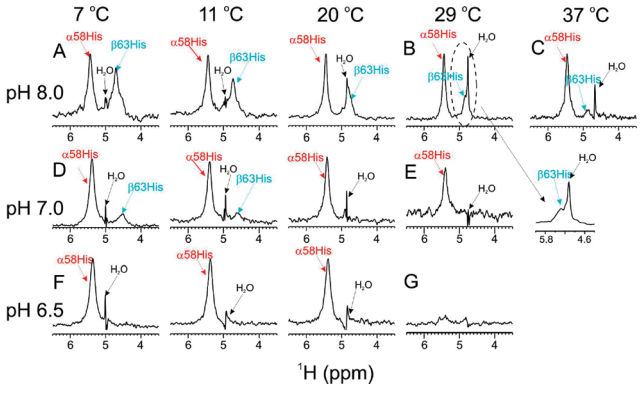

FIGURE 2: Horizontal 1D slices along the ^{1}H axis through the cross-peak of the side chain of β63His extracted from 600 MHz (^{1}H,^{15}N) HSQC spectra of fully ^{15}N-labeled $rHbO_2$ A in H_2O under various conditions of pH and temperature. The panels are marked with the same letter as the corresponding panels (pH, temperature) from Figure 1.

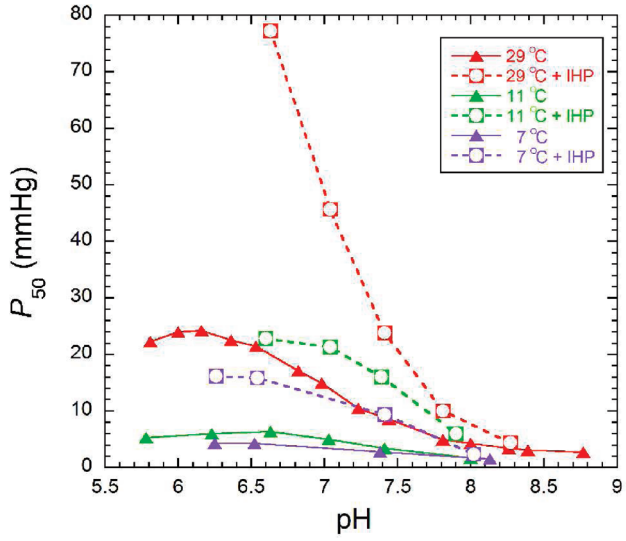

FIGURE 3: Oxygen-binding properties of Hb A as a function of pH at 29 °C (red), 11 °C (green), and 7 °C (magenta) in 0.1 M sodium phosphate buffer without IHP (filled triangles) and with 4 times molar concentration of IHP (open circles).

temperature on the stability of the H-bond marker has been examined in the range from 7 to 37 °C and at different pH values. At pH 8.0 and 29 °C, the cross-peaks for both α58His (^{1}Hε_2, ^{15}Nε_2) and β63His (^{1}Hε_2, ^{15}Nε_2) are clearly visible, but that for β63His is weaker (Figures 1B and 2B). When the temperature is increased to 37 °C, the peak of β63His (^{1}Hε_2, ^{15}Nε_2) becomes very weak but still observable (Figures 1C and 2C), and when the temperature is decreased to 7 °C, this peak becomes much stronger (Figures 1A and 2A). At pH 7.0, the cross-peak for β63His (^{1}Hε_2, ^{15}Nε_2) is missing at 29 °C (Figures 1E and 2E) but is clearly seen at 7 °C (Figures 1D and 2D), while the cross-peak for α58His (^{1}Hε_2, ^{15}Nε_2) is visible at all temperatures shown, and its intensity decreases at higher temperatures. At the lowest pH,

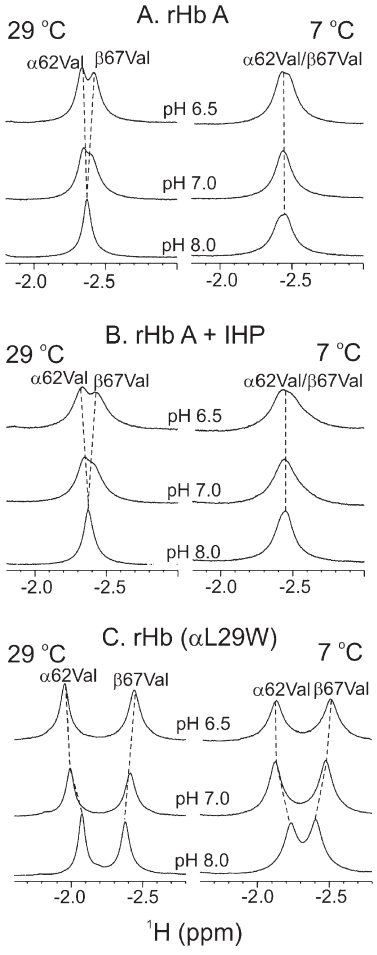

FIGURE 4: Ring-current-shifted proton resonances in ^{1}H NMR spectra (600 MHz) of rHbO_2 A in the absence and presence of IHP (A and B) and mutant rHbO_2 (αL29W) (C) in 95% H_2O, 5% D_2O, 0.1 M sodium phosphate buffer at different pH (8.0, 7.0, and 6.5) and temperatures (29 and 7 °C), respectively.

pH 6.5, the cross-peak for α58His ($^1H\varepsilon_2$, $^{15}N\varepsilon_2$) is missing at 29 °C (Figures 1G and 2G) but appears at 7 °C (Figures 1F and 2F). However, at pH 6.5, the cross-peak for β63His ($^1H\varepsilon_2$, $^{15}N\varepsilon_2$) is undetectable even at 7 °C (Figures 1F and 2F).

Figure 4 shows the nonexchangeable ring-current-shifted proton resonances from −1 to −3 ppm from DSS. These resonances provide valuable information about the environment in the heme pockets. On the basis of our previous studies, the resonances at −1.75 and −1.82 ppm in the spectra of HbCO A at 29 °C (results not shown) have been assigned to the γ_2-CH_3 group of the α62Val and β67Val (E11), respectively (*18*, *19*). In rHbO_2 A at 29 °C, the ring-current-shifted resonances from α62Val and β67Val occur around −2.4 ppm, are overlapped at pH 8.0, and become clearly resolved at pH 6.5. However, at 7 °C, these two peaks shift only slightly from pH 8.0 to pH 6.5 (Figure 4A,B). This is consistent with the changes in the intensity of the distal H-bond markers under different pH and temperature conditions. For example, the H-bond markers for the α-heme pockets change significantly at 29 °C (Figure 1B,E,G) and change only slightly at 7 °C (Figure 1A,D,F). As shown in Figure 3, the Bohr effect is also dramatically affected by temperature. At 29 °C, the P_{50} value increases about 7-fold between pH 6.0 (21.5 mmHg) and pH 8.4 (3.1 mmHg) but changes much less at 7 °C between pH 6.5 (4.3 mmHg) and pH 8.1 (1.5 mmHg). Thus, the changes in the chemical shifts of the E11 valyl residues and the intensity of the H-bond markers are consistent with the effects of pH and temperature on the oxygen-binding affinity.

Effect of IHP. A number of studies have been reported regarding the functional changes induced by organic phosphates, e.g., 2,3-bisphosphoglycerate (2,3-BPG) and IHP, in Hb A and mutant Hbs (*12*, *13*, *20*). On the basis of the X-ray crystallographic studies, 2,3-BPG and IHP are believed to bind to the central cavity, between the two β-chains of the Hb molecule in the deoxy form, and thus stabilize the deoxy quaternary structure and lower the oxygen affinity (*21*−*24*). On the other hand, molecular dynamics simulations suggest that allosteric effectors, such as 2,3-BPG, bezafibrate (BZF), and IHP, affect only the ligation-linked tertiary structural changes rather than the homotropic ligation-linked T → R quaternary structural transition (*25*−*27*).

In our study, the oxygen-binding affinity for rHb A is measured in the presence of IHP under different conditions of pH (pH 8.0, 7.0, and 6.5) and temperature (29, 11, and 7 °C). As shown in Figure 3, at lower pH and/or higher temperature, IHP has a greater effect on the oxygen binding. When the oxygen-binding affinity is highest at high pH (pH 8.0), the P_{50} values do not change significantly upon the addition of IHP. The effect of IHP on P_{50} becomes obvious when the pH is lower than 7.5 and when the temperature is higher. At pH 7.0 and 29 °C, the P_{50} values for Hb A with and without IHP are 45.7 and 15.0 mmHg, whereas at 11 °C the values are 21.3 and 5.0 mmHg, respectively (Figure 3). In order to investigate if the H-bond marker would be affected by the addition of IHP, HSQC spectra were collected under each of the corresponding experimental conditions. It is found that upon the addition of IHP, the H-bond marker for the α-heme pocket, the cross-peak of α58His ($^1H\varepsilon_2$, $^{15}N\varepsilon_2$), does not change significantly and that for the β-heme pocket becomes weaker at pH 8.0 and 7 °C and disappears under the other conditions (Figure 5). Looking at the ring-current-shifted resonances shown in Figure 4A,B, the changes in the chemical shifts of α62Val and β67Val due to the temperature and pH are also quite similar in the presence and absence of IHP. IHP slightly perturbs the position of the E11 valyl residue in the β-heme pocket (Figure 4B), consistent with the previous findings (*18*, *19*).

Mutations in the $\alpha_1\beta_1$ and $\alpha_1\beta_2$ Interfaces. It is well-known that mutations in the $\alpha_1\beta_2$ subunit interfaces of Hb A can significantly change the oxygen affinity (*1*, *28*). For example, Hb Kempesy (βD99N) is a naturally occurring mutant of Hb A with high oxygen affinity and very low cooperativity (*29*). The functional defect for Hb Kempsey is believed to be due to the substitution of Asn for Asp at β99, which prevents the formation of an important intersubunit H-bond between α42Tyr and β99Asp in the T-state. This structural change destabilizes the T-state of Hb Kempesy, thus causing an increase in the oxygen-binding affinity. In contrast, rHb (αV96W) was designed as a low-oxygen affinity mutant by introducing a new water-mediated H-bond between the indole nitrogen atom of α96Trp and β101Glu across the T-state interface (*12*, *30*). Thus, it would be interesting to know whether the H-bond markers in the distal heme pockets would be affected by the mutation in the subunit interfaces of Hb A. Four rHbs with mutations in the $\alpha_1\beta_2$ and/or $\alpha_1\beta_1$ interfaces of Hb A were selected to examine this correlation. The NMR results show that the H-bond markers for the α-heme pocket in a low-affinity mutant, rHb (αV96W) (Figure 6A,B), and a high-affinity mutant, rHb Kempesy (βD99N) (Figure 6C,D), exhibit a pattern similar to that observed for rHb A, i.e., showing a stronger signal at high pH and/or low temperature and a weaker

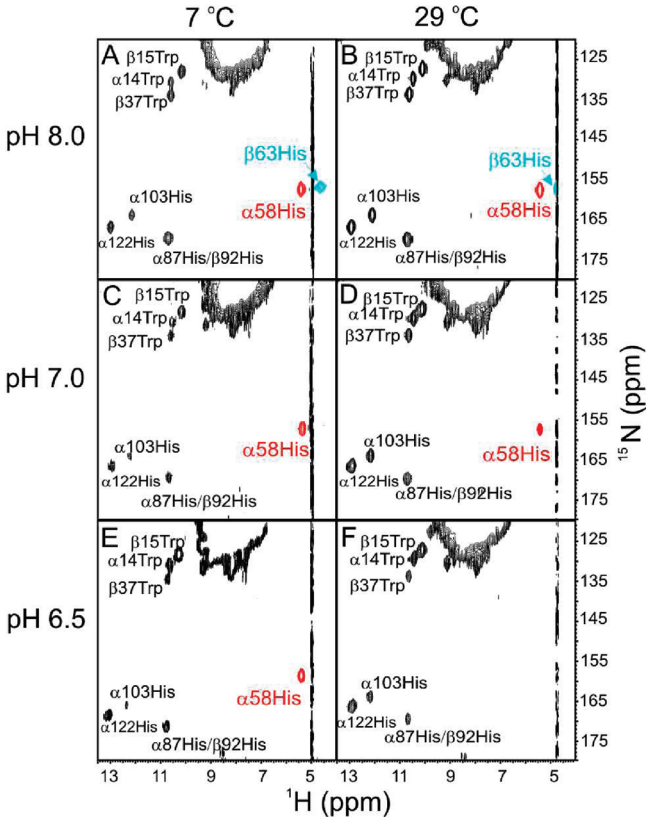

FIGURE 5: His and Trp side-chain regions of 600 MHz (^{1}H,^{15}N) HSQC spectra of fully ^{15}N-labeled HbO_2 A in H_2O in the presence of IHP at pH 8.0 (upper row), pH 7.0 (middle row), and pH 6.5 (lower row) and, by columns, at 7 °C (left) and 29 °C (right), respectively. The cross-peaks for the relevant directly bonded ^{15}N−^{1}H pairs are labeled.

signal at low pH and/or high temperature. The H-bond marker for the β-heme pocket, the cross-peak of β63His ($^{1}H\varepsilon_2$, $^{15}N\varepsilon_2$), also exhibits similar behavior as in rHb A, except that the cross-peak does not appear at pH 7.0 and 7 °C.

Further examination of the H-bond markers has been carried out on a compensatory mutant for Hb Kempsey, rHb (αY42D/βD99N), which was designed to restore its functional properties by providing an alternate H-bond to replace the one that is missing in Hb Kempsey (*11*). The H-bond cross-peaks for this mutant rHb exhibit a very similar pattern compared to that for rHb A at all experimental conditions (pH and temperature) (Figure 6E, F).

Another mutant tested in this study, rHb (αV96W/βN108K), has the greatest tendency to switch to the T-type structure, even when it is still in the ligated state (*13*). The mutation at β108 (G10) Asn → Lys is located in the $\alpha_1\beta_1$ subunit interface in the central cavity of the Hb molecule (*1*). The combination of mutations in the $\alpha_1\beta_1$ and $\alpha_1\beta_2$ interfaces produced a mutant with good cooperativity and the lowest oxygen affinity among the hemoglobins designed in our laboratory. There are two cross-peaks, at 12.9 and 12.1 ppm proton chemical shift, which have been assigned to the side-chain $N\varepsilon_2H$ group of α122His and α103His, H-bonded to β35Tyr and β131Gln, respectively, in the $\alpha_1\beta_1$ interface (*15*, *31*, *32*). At pH 8.0, these cross-peaks are very weak at 7 °C and missing at 29 °C (Figure 7), suggesting that the $\alpha_1\beta_1$ interface is disturbed by the mutation at β108 as observed from the previous study for other $\alpha_1\beta_1$ interface mutants (*13*, *32*). However, the H-bond markers from both α58His and β63His are clearly visible at 7 °C and still can be observed at 29 °C (Figure 7),

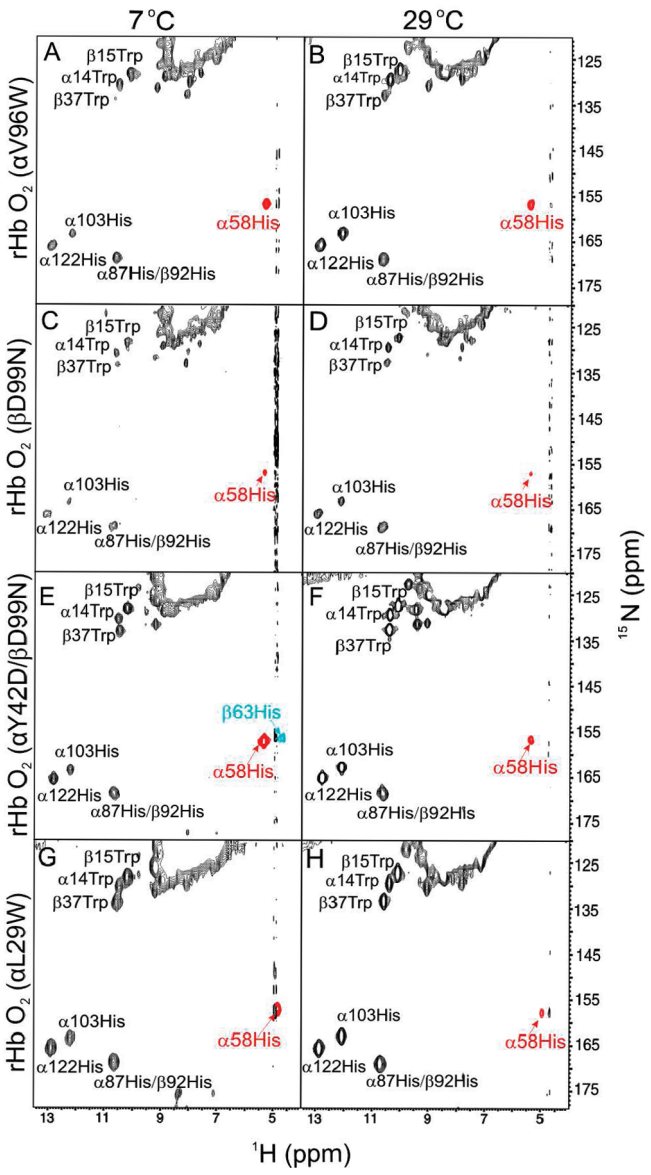

FIGURE 6: His and Trp side-chain regions of 600 MHz (^{1}H,^{15}N) HSQC spectra of fully ^{15}N-labeled mutant $rHbO_2$ (αV96W) (A and B), $rHbO_2$ (βD99N) (C and D), $rHbO_2$ (αY42D/βD99N) (E and F), and $rHbO_2$ (αL29W) (G and H) in 95% H_2O, 5% D_2O, 0.1 M sodium phosphate buffer at pH 7.0, 7 °C (left column) and 29 °C (right column), respectively. The cross-peaks for directly bonded ^{15}N−^{1}H of the relevant side chains are labeled.

similar to those seen for rHb A. This result clearly suggests that although the quaternary structure is affected by the mutation in the subunit interfaces, the conformation of the heme pocket does not appear to change significantly and shows that the affinity for oxygen is controlled by multiple mechanisms involving quaternary and tertiary structural effects as well as the dynamics of this complicated molecule (*33*).

The effect of IHP has also been examined for the low-affinity mutant, $rHbO_2$ (αV96W/βN108K), and the high-affinity mutant, $rHbO_2$ (αY42D/βD99N), by carrying out the HSQC experiments in the presence of IHP. Our results show that the H-bond markers in the distal heme pocket of these two mutants do not change significantly upon binding with IHP (Supporting Information Figure 1S). This is consistent with the results observed for rHb A in the oxy form.

Mutation in the Distal Heme Pocket. Our previous studies involving the mutations at the B10 position in Hb A have shown

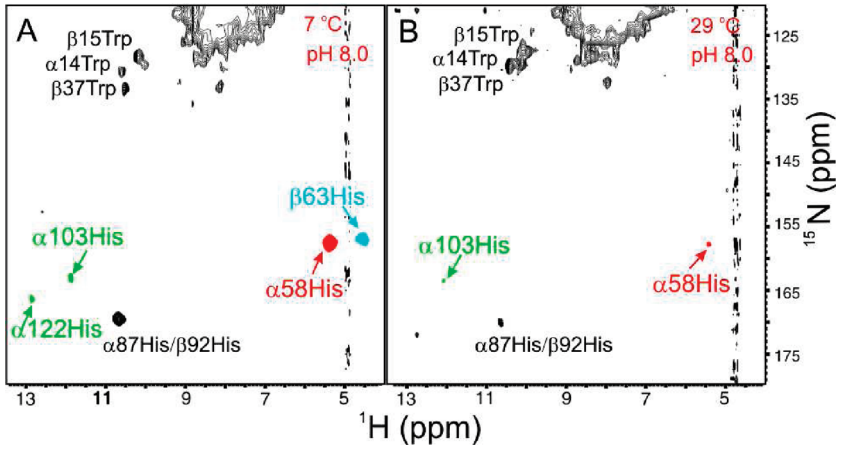

FIGURE 7: His and Trp side-chain regions of 600 MHz (^{1}H,^{15}N) HSQC spectra of fully ^{15}N-labeled mutant rHbO$_2$ (αV96W/βN108K) in H$_2$O at pH 8.0, 7 °C (left) and 29 °C (right), respectively. The cross-peaks for directly bonded ^{15}N−^{1}H of the relevant side chains are labeled.

that rHb (αL29W), rHb (*β*L28F), and rHb (*β*L28W) exhibit very low oxygen affinity and reduced cooperativity compared to those of Hb A, while rHb (αL29F) exhibits high oxygen affinity (*14*, *33*). Proton NMR spectroscopy indicates that these mutations in the B10 helix do not perturb the $\alpha_1\beta_1$ and $\alpha_1\beta_2$ subunit interfaces significantly (an expected result), while the tertiary structures near the heme pockets are affected. rHb (αL29W) was chosen for the present study, and the HSQC experiments were performed for this mutant in the oxy form to test if the H-bond would be affected. At pH 8.0, both of the H-bond markers for the α- and *β*-chains can be observed at 29 °C (Supporting Information Figure 1S) with similar peak intensities as those shown for rHbO$_2$ A. The most significant change detected under this experimental condition is that the cross-peak of α58His (^{1}Hε_2, ^{15}Nε_2) is shifted upfield by about 0.2 ppm, suggesting that the local environment is changed by the mutation in the distal heme pocket of the α-chain. On the basis of our previous study, the difference in the oxygen-binding affinity between rHb (αL29W) and Hb A becomes larger at lower pH. At pH 7.0 and 29 °C, the P_{50} value for this mutant is about 50 mmHg, which is much higher than that for Hb A (15.1 mmHg) (*14*, *33*), indicating a more substantial decrease in the oxygen affinity. Thus, more significant differences in the H-bond markers are expected to be observed at the lower pH. Indeed, at pH 7.0 and 29 °C, the H-bond marker for the α-heme pocket of rHb (αL29W) is much weaker than that in rHb A under the same experimental condition but can still be observed (Figure 6H). Meanwhile, the pattern of the H-bond marker for the *β*-heme pocket does not change significantly compared to that of rHb A. The same experiment was carried out at 20, 11, and 7 °C to confirm that the mutation in the distal heme pocket does make the H-bond marker of the α-chain weaker (Supporting Information Figure 1S). Figure 4C shows that the resonance of α62Val moves downfield, and changes due to experimental conditions are easily observed. Thus, the mutation in the α-heme pocket decreases the binding affinity by changing the geometry of the distal heme pocket, as demonstrated by the H-bond markers and the chemical shift of the valyl residue.

DISCUSSION

Changes in the Heme Pockets Due to the Ligation States. The X-ray crystal structures of Hb A in deoxy, oxy, and carbonmonoxy forms determined at 1.25 Å resolution have provided a detailed structural model for hemoglobin (*4*). As shown in Figure 8, the geometry of the heme pockets changes

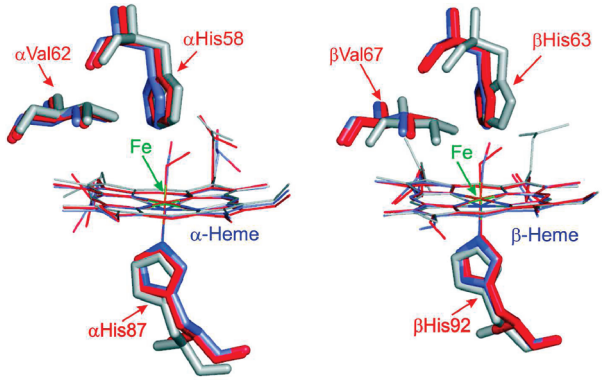

FIGURE 8: Individual heme pockets in the α- and *β*-subunits of oxy-, CO-, and deoxy-Hb A with hemes superimposed, colored red for HbO$_2$ A, blue for HbCO A, and gray for deoxy-Hb A, respectively. The Fe atom in the heme is colored green for HbO$_2$ A, yellow for HbCO A, and blue for deoxy-Hb A, respectively. Illustrations of the Hb A structure produced by using the graphics program PyMOL (*51*). Coordinates of Hb A in the oxy, CO, and deoxy forms were obtained from Brookhaven Protein Data Bank files 2DN1, 2DN3, and 2DN2, respectively.

upon ligand binding, but the major change is in the heme plane. If the structures of HbO$_2$ A (PDB code 2DN1) and deoxy-Hb A (PDB code 2DN2) are superimposed based on the four nitrogen atoms of the heme, the heme planes fit very well, with the iron atom in the plane in the ligated states, but the iron atom moves down 0.45 Å to a domed heme conformation in the unligated state. In the distal heme pocket, the E11 valyl residues move forward toward the heme in the deoxy form of Hb A. A more significant movement is observed for *β*67Val than for α62Val. Meanwhile, the $\alpha_1\beta_1$ and $\alpha_2\beta_2$ dimers shift slightly and rotate by about 11° with respect to each other. Thus, there are two major structural changes upon ligand binding, i.e., the reorientation of the $\alpha_1\beta_1$ and $\alpha_2\beta_2$ dimers and the movement of the iron atom with respect to the heme plane.

The formation of a H-bond between the distal histidine side-chain NH and the oxygen bound to the heme iron is believed to be the explanation for the increased relative binding affinity for oxygen versus CO in the heme proteins (myoglobin and hemoglobin). This H-bond stabilizes the NH group against the exchange with the water solvent and thus makes possible to observe the one-bond scalar coupling between ^{1}H and ^{15}N (about 95 Hz), manifested as a doublet with the corresponding separation equal to $^1J_{NH}$ in the 1D spectra or as a cross-peak in the 2D

HSQC or HMQC spectra. If the histidyl NH proton is able to participate in a solvent proton exchange, the intensity of the cross-peak diminishes if the exchange rate is lower than $^1J_{NH}$ and disappears when the exchange is faster (*9*). This is why of the 19 histidine residues per $\alpha\beta$ dimer that we only observe the side-chain NH cross-peaks for the two histidines in the $\alpha_1\beta_1$ interface (α103 and α122) in all ligation forms and for the distal histidines (α and β) only in the oxy form. We also see the HδN cross-peak of the α- and β-proximal histidines in the diamagnetic CO and oxy forms. The H-bond between the distal histidine and the O_2 ligand is a sensitive marker for the changes in the heme pocket and is directly related to the change in the oxygen affinity. The disappearance or the weakening of the H-bond marker (intensity) means that the ligand is likely to be released from the heme. Our studies have shown that both pH and temperature can change the O_2 binding affinity of Hb A and also affect the H-bond markers directly. On the other hand, the mutations in the subunit interface and/or organic phosphate have a much weaker effect on the H-bond markers, suggesting that these structural perturbations may have major effects on the quaternary structure of Hb A, but only indirectly affect the tertiary structure of the distal heme pocket.

H-Bond Markers and Changes in the Oxygen-Binding Affinity. On the basis of previous studies, there are many factors, such as pH and temperature, that affect the oxygen binding to Hb. The H^+ ion is a known heterotropic allosteric effector in the oxygenation of Hb. As shown in Figure 3, the oxygen affinity of Hb A strongly depends on pH, and this dependence is known as the Bohr effect (*1*). This physiologic effect is fundamentally important in the ability of the Hb molecule to deliver O_2 to the tissues, particularly to working muscles, where lactic acid is produced and the pH is thus lower. As suggested by the X-ray crystallographic results and then confirmed by our NMR findings, the binding of O_2 to Hb is stabilized by the H-bonds between oxygen and distal histidines (*4*, *9*). Using NMR spectroscopy, we have found that the changes in these H-bonds are correlated with the changes in the O_2-binding affinity brought upon by pH and/or temperature. At lower pH or higher temperature, the O_2-binding affinity is lower than at high pH and low temperature. Meanwhile, the H-bond markers become weaker, suggesting that under these conditions the side chains of the distal histidines experience an increased mobility so that the proton exchange with a water molecule in the distal heme pocket is faster. Thus, the oxygen molecule would be correspondingly less stabilized by the H-bond and become easier to be released, which is consistent with the changes in the O_2 affinity of Hb. This H-bond marker can also show the subtle difference between the α- and β-distal-heme pockets. On the basis of our previous NMR studies, the α-subunit has a higher O_2-binding affinity than the β-subunit in the presence of organic phosphate (*34*, *35*). The X-ray crystal structures indicate that the oxygen ligand and distal histidine in the α-heme pocket have a more favorable geometry to form a H-bond than that in the β-heme pocket (*4*). NMR experiments in our study have confirmed that the H-bond between β63His and oxygen is weaker and more sensitive to changes in pH and temperature. The weaker H-bond in the β-heme pocket is illustrated by the much smaller intensity of its corresponding cross-peak as compared to that of the α-heme pocket (see Figures 1 and 2) under all experimental conditions investigated in this work. It also tends to disappear in most situations when the oxygen affinity is lower.

Effect of IHP on the Structure of Hb A. It is known that allosteric effectors, such as hydrogen ions, chloride ions, and organic phosphates, e.g., 2,3-BPG and IHP, modulate the oxygen affinity of hemoglobin. However, the role of IHP with respect to oxygen binding in hemoglobin is controversial. Previous studies based on the backbone dynamics show a conformational fluctuation of HbCO A upon IHP binding, especially at the interdimer interfaces and affecting the α- and β-subunits differently (*36*). The major conformational changes during the Hb allosteric transition can be attributed to the sliding contacts in the areas including the $\alpha_1\beta_2$ or $\alpha_2\beta_1$ interface, especially in the switch region (αC helix-βFG corner), the joint region (βC helix-αFG corner), and the carboxy terminals of both α- and β-chains (*36*). The fluctuation might shift the averaged solution quaternary structure of IHP-bound HbCO A slightly toward the R structure from the midpoint between the R and R2 structures, as suggested by NMR residual dipolar coupling (RDC) experiments for HbCO A and mutant rHbCO (αV96W) in the presence of IHP (*37*). Yonetani et al. (*25*) have advocated a global allostery model based on molecular dynamics simulation for hemoglobin. Their model proposes that the oxygen affinities of the T- (low-affinity) and R- (high-affinity) functional states of Hb are changed by heterotropic effector-linked tertiary structural changes without changing the respective T (deoxy)- and R (oxy)-quaternary states. Our previous studies have shown that the side chain of β37Trp residue is a sensitive marker for the quaternary structural and dynamic changes in the $\alpha_1\beta_2$ ($\alpha_2\beta_1$) interface caused by IHP (*38*). In the experiments reported here, the H-bonds between the bound O_2 and the distal histidyl residues in the α- and β-heme pockets are used as markers to investigate if there are any tertiary structural changes upon the addition of IHP. The results show that while IHP affects the oxygen-binding affinity significantly, it has a lesser effect on the H-bond markers. For example, at pH 7.2 and 29 °C in 0.1 M phosphate, the P_{50} value for Hb A is 10.5 and 46.7 mmHg in the absence and presence of IHP, respectively, indicating that the oxygen-binding affinity changes significantly (4-fold) upon the addition of IHP (Figure 3). Under similar experimental conditions, the H-bond marker in the α-heme pocket is only slightly affected (see Figures 1E and 5D). The different effects on the O_2-binding affinity and the H-bond marker can also be observed for a compensatory mutant rHb (αY42D/βD99N). At 29 °C and pH 7.2 in 0.1 M phosphate, the oxygen affinity is decreased about 5-fold (P_{50} value of 2.5 mmHg without IHP and 12.9 mmHg with IHP) (*11*). The H-bond marker in the α-heme pocket can be observed under both conditions (Supporting Information Figure 1S). Thus, the NMR results reported here suggest that the change in the oxygen-binding affinity is mainly due to the quaternary structural perturbation upon the addition of IHP, although there is a contribution from a perturbation of the dynamics of the β-chain (see below).

Our recent studies of the backbone dynamics and RDC measurements show that, in general, IHP affects the α- and β-subunits of Hb A differently (*36*, *37*). These differences can also be observed for the H-bond markers. For example, at pH 7.0 in 0.1 M phosphate, the H-bond marker of the α-heme pocket shows up clearly even in the presence of IHP (Figure 5C,D) at all temperatures. But the H-bond marker of the β-heme pocket, which is already weak at pH 7.0 and at 7 °C in the absence of IHP (Figure 1D), disappears upon adding IHP (Figure 5C,D), suggesting that this H-bond is more fragile and is more sensitive to the perturbation by IHP. This result also suggests that the presence of IHP does have an effect on the tertiary structure of

Hb A, although this effect may be caused indirectly by its perturbation to the quaternary structure. The recent results are consistent with our earlier studies that IHP exerts its effects on both the tertiary and quaternary structures of Hb A (*36*, *37*, *39*).

H-Bond Markers and Structural Changes Induced by Mutations. It is well-known that mutations either in the interfaces or in the heme pocket of hemoglobin can significantly change the oxygen-binding affinity. In our studies, when the mutation is made in the α-heme pocket, changes in the H-bond markers and chemical shifts of the valyl residues are observed, suggesting that the affinity changes are related to a geometric change of the α-heme pocket. On the other hand, the mutations at the $\alpha_1\beta_2$ (or $\alpha_2\beta_1$) interface change the O_2-binding affinity by shifting the equilibrium between the R- and the T-states of these rHb mutants toward the T-state (low-affinity) geometry or the R-state (high-affinity) geometry (*11*−*14*). While having more significant effects on the quaternary structure, the mutations at this interface also affect the structure of the heme pockets, which can be suggested by the weaker H-bond markers for the *β*-chain of both low- and high-oxygen affinity mutants (Figure 6A,C). However, for those mutations in the subunit interfaces, the H-bonds for the α-chain appear to be less affected. Since the high-affinity mutants, such as rHb Kempesy and its compensatory mutant rHb (αY42D/*β*D99N), prefer to remain in the ligated state, it is understandable that the H-bond markers of these mutants are less affected. For low-affinity mutants, such as rHb (αV96W) and rHb (αV96W/*β*N108K), the switching between the R-state and the T-state can occur easily; namely, the appearance of the T-state marker is observed at 14 ppm in ^{1}H NMR spectra while these rHbs are in the ligated state (*12*, *13*), especially at lower temperatures. The T-state marker has been previously (*40*) identified as the intersubunit H-bond between α42Tyr and *β*99Asp in the $\alpha_1\beta_2$ interface in deoxy-Hb A, and it is very sensitive to the quaternary structural switching between the R- and the T-states. On the other hand, the H-bond markers in the distal heme pockets are not affected significantly (Figure 7A) at 7 °C. This proves that hemoglobin is in the ligated state and suggests that the tertiary structure of the α-distal heme pocket is quite robust with respect to the perturbations from the subunit interface. At higher temperatures, though, both distal heme pockets become more dynamic, and the cross-peaks diminish and even disappear (Figure 7B).

Our present study suggests that the H-bond between ligand O_2 and distal histidines can be used as a sensitive marker for change in the ligation state. For the mutants, it is possible that the two dimers ($\alpha_1\beta_1$ and $\alpha_2\beta_2$) could start to switch the quaternary structure even before the ligation states change. For the low-affinity mutants in the CO form in the presence of IHP and/or lowering the temperature, this could be the reason that the T-state markers in the $\alpha_1\beta_2$ interface can be observed without the ligands leaving the heme.

Dynamic Ensemble of Hemoglobin Structures in Solution. There are at least four R-type ligated Hb A and nine T-type deoxy-Hb A crystallized under different temperature, pH, buffer, and salt conditions (*4*, *6*, *41*−*50*). Using the graphics program PyMOL (*51*), the X-ray crystal structure of HbO_2 A (PDB code 2DN1) was superimposed on that of deoxy-Hb A (PDB code 2DN2), and the root-mean-square deviation (rmsd) value was 2.412 Å based on 570 Cα atoms of the tetramer but only 0.894 Å when based on 285 Cα atoms of the $\alpha_1\beta_1$ (or $\alpha_2\beta_2$) dimer. This suggests that the major structural changes upon ligand binding are in the $\alpha_1\beta_2$ (or $\alpha_2\beta_1$) subunit interface, involving several salt bridges and H-bonds. Meanwhile, the $\alpha_1\beta_1$ (or $\alpha_2\beta_2$) dimer behaves as a rigid body, whose overall structure is essentially insensitive to ligation (*52*). Further comparisons have been carried out for different R-type or T-type structures of hemoglobin. The rmsd for the four R-type structures is 1.7−1.9 Å based on the tetramer but is only 0.8−0.9 Å based on the dimer. There is no significant structural difference shown in the heme pocket based on the superimposition of $\alpha_1\beta_1$ (or $\alpha_2\beta_2$) dimers, suggesting that the major differences between these R-type structures are coming from the differences in the interdimer, i.e., $\alpha_1\beta_2$ (or $\alpha_2\beta_1$), interface. Meanwhile, for the nine deoxy-form (T-type) structures, the difference between the tetramers is much smaller on the basis of the rmsd values ranging from 0.1 to 0.4 Å, suggesting that the $\alpha_1\beta_2$ (or $\alpha_2\beta_1$) interfaces exhibit less variance in the unligated form.

It has been suggested that the interdimer $\alpha_1\beta_2$ (or $\alpha_2\beta_1$) subunit interface in ligated Hb A has a weaker interaction than that in the intradimer $\alpha_1\beta_1$ (or $\alpha_2\beta_2$) interface (*52*−*54*) and that the interaction in the $\alpha_1\beta_2$ (or $\alpha_2\beta_1$) subunit becomes stronger in the unligated form of Hb A with the formation of several H-bonds and salt bridges (*55*). Thus, in the ligated form of Hb A, the $\alpha_1\beta_2$ or $\alpha_2\beta_1$ interface is more relaxed and more dynamic and is more easily affected by environmental conditions, such as pH, mutations, and organic phosphate. Our previous studies have shown that most of the backbone residues of Hb A are rigid on the time scale of nanoseconds to picoseconds (*36*, *56*), which is much faster than the time scale of domain reorientation that is the basis of hemoglobin's flexibility. The experimentally determined RDC values can be well reproduced by calculations based on either of the X-ray structures for isolated α- or *β*-chain or that of an isolated αβ dimer. However, a larger χ^2 value is obtained when based on the whole tetramer (*39*, *57*). For HbCO A, a better fitting is obtained by a rotation of one αβ dimer with respect to the other (*57*). Thus, the X-ray crystal structure may only be a snapshot of basically identical $\alpha_1\beta_1$ and $\alpha_2\beta_2$ dimers, with a particular tetramer−dimer interface. Which kind of interface can be observed in the X-ray crystal structure appears to depend on the experimental conditions used for crystallization. Since these interdimer interfaces are "relaxed" in the ligated form of Hb A, the structure of the ligated hemoglobin in solution appears to be an ensemble of two αβ dimers with dynamic $\alpha_1\beta_2$ and $\alpha_2\beta_1$ subunit interfaces, i.e, a dynamic ensemble of various quaternary structures.

CONCLUSION

Ligand binding to hemoglobin is a dynamic and synergistic process involving many tertiary and quaternary structural changes. The cross-peaks of α58His ($^1H\varepsilon_2$, $^{15}N\varepsilon_2$) and *β*63His ($^1H\varepsilon_2$, $^{15}N\varepsilon_2$) side chains in Hb A can be used as the H-bond markers to reflect structural and dynamic changes in the distal heme pocket under various experimental conditions in solution. Our results show that the stability of these H-bonds is sensitive to changes in pH and temperature, which are key effectors in regulating the oxygen-binding affinity of Hb and affect the heme pocket directly. Mutations in the subunit interface can also change the oxygen-binding affinity by shifting the equilibrium between R-type and T-type structures but may not have a direct effect on the distal heme pocket. Our results show that two allosteric effectors, H^+ ion and IHP, exert different effects on the structure and function of the Hb molecule. Using the distal

histidine H-bond as a marker, we are able to illustrate how the oxygen-binding affinity of hemoglobin is affected by different effectors in solution and also provide a better view of the changes in the distal heme pocket upon ligand binding. The stability of the distal H-bonds against perturbation by mutations and allosteric effectors suggests that hemoglobin in the ligated form is a dynamic ensemble consisting of two rigid $\alpha_1\beta_1$ and $\alpha_2\beta_2$ dimers with relaxed but also dynamic $\alpha_1\beta_2$ or $\alpha_2\beta_1$ interface. The structural features of the $\alpha_1\beta_2$ and $\alpha_2\beta_1$ interfaces are dependent on the environmental conditions and can indirectly affect the oxygen-binding affinity.

ACKNOWLEDGMENT

We thank Ms. Tsuey Chyi S. Tam for assistance in the preparation of the recombinant hemoglobin samples used in this study.

SUPPORTING INFORMATION AVAILABLE

Figure 1S showing the histidine side chain region of 600 MHz (^1H,^{15}N) HSQC spectra of fully ^{15}N-labeled normal and mutant rHbs in the oxy form in H_2O under various experimental conditions. This material is available free of charge via the Internet at http://pubs.acs.org.

REFERENCES

1. Dickerson, R. E., and Geis, I. (1983) Hemoglobin: Structure, Function, Evolution, and Pathology, Benjamin/Cummings, Menlo Park, CA.
2. Olson, J. S., and Phillips, G. N. (1997) Myoglobin discriminates between O_2, NO, and CO by electrostatic interactions with the bound ligand. *J. Biol. Inorg. Chem. 2*, 544–552.
3. Shaanan, B. (1983) Structure of human oxyhemoglobin at 2.1 Å resolution. *J. Mol. Biol. 171*, 31–59.
4. Park, S.-Y., Yokoyama, T., Shibayama, N., Shiro, Y., and Tame, J. R. H. (2006) 1.25 Å resolution crystal structures of human haemoglobin in the oxy, deoxy and carbonmonoxy forms. *J. Mol. Biol. 360*, 690–701.
5. Ackers, G. K. (1998) Deciphering the molecular code of hemoglobin allostery. *Adv. Protein Chem.* 185–253.
6. Chan, N. L., Kavanaugh, J. S., Rogers, P. H., and Arnone, A. (2004) Crystallographic analysis of the interaction of nitric oxide with quaternary-T human hemoglobin. *Biochemistry 43*, 118–132.
7. Shibayama, N., Morimoto, H., and Saigo, S. (1998) Asymmetric cyanomet valency hybrid hemoglobin, ($\alpha^{+CN^-}\beta^{+CN^-}$)($\alpha\beta$): The issue of valency exchange. *Biochemistry 37*, 6221–6228.
8. Eaton, W. A., Henry, E. R., Hofrichter, J., and Mozzarelli, A. (1999) Is cooperative oxygen binding by hemoglobin really understood? *Nat. Struct. Biol. 6*, 351–358.
9. Lukin, J. A., Simplaceanu, V., Zou, M., Ho, N. T., and Ho, C. (2000) NMR reveals hydrogen bonds between oxygen and distal histidines in oxyhemoglobin. *Proc. Natl. Acad. Sci. U.S.A. 97*, 10354–10358.
10. Shen, T. J., Ho, N. T., Simplaceanu, V., Zou, M., Green, B. N., Tam, M. F., and Ho, C. (1993) Production of unmodified human adult hemoglobin in *Escherichia coli*. *Proc. Natl. Acad. Sci. U.S.A. 90*, 8108–8112.
11. Kim, H. W., Shen, T. J., Sun, D. P., Ho, N. T., Madrid, M., Tam, M. F., Zou, M., Cottam, P. F., and Ho, C. (1994) Restoring allosterism with compensatory mutations in hemoglobin. *Proc. Natl. Acad. Sci. U.S.A. 91*, 11547–11551.
12. Kim, H. W., Shen, T. J., Sun, D. P., Ho, N. T., Madrid, M., and Ho, C. (1995) A novel low-oxygen affinity recombinant hemoglobin (α96Val→Trp)—Switching quaternary structure without changing the ligation state. *J. Mol. Biol. 248*, 867–882.
13. Tsai, C. H., Shen, T. J., Ho, N. T., and Ho, C. (1999) Effects of substitutions of lysine and aspartic acid for asparagine at β108 and of tryptophan for valine at α96 on the structural and functional properties of human normal adult hemoglobin: Roles of $\alpha_1\beta_1$ and $\alpha_1\beta_2$ subunit interfaces in the cooperative oxygenation process. *Biochemistry 38*, 8751–8761.
14. Wiltrout, M. E., Giovannelli, J. L., Simplaceanu, V., Lukin, J. A., Ho, N. T., and Ho, C. (2005) A biophysical investigation of recombinant hemoglobins with aromatic B10 mutations in the distal heme pockets. *Biochemistry 44*, 7207–7217.
15. Simplaceanu, V., Lukin, J. A., Fang, T. Y., Zou, M., Ho, N. T., and Ho, C. (2000) Chain-selective isotopic labeling for NMR studies of large multimeric proteins: Application to hemoglobin. *Biophys. J. 79*, 1146–1154.
16. Davis, A. L., Keeler, J., Laue, E. D., and Moskau, D. (1992) Experiments for recording pure-absorption heteronuclear correlation spectra using pulsed field gradients. *J. Magn. Reson. 98*, 207–216.
17. Doyle, M. L., Gill, S. J., Decristofaro, R., Castagnola, M., and Dicera, E. (1989) Temperature-dependence and pH-dependence of the oxygen-binding reaction of human-fetal hemoglobin. *Biochem. J. 260*, 617–619.
18. Lindstrom, T. R., Lehmann, H., Charache, S., Noren, I. B. E., and Ho, C. (1972) Nuclear magnetic resonance studies of hemoglobins. 7. Tertiary structure around ligand binding-site in carbonmonoxyhemoglobin. *Biochemistry 11*, 1677–1681.
19. Dalvit, C., and Ho, C. (1985) Proton nuclear Overhauser effect investigation of the heme pockets in ligated hemoglobin—Conformational differences between oxy and carbonmonoxy forms. *Biochemistry 24*, 3398–3407.
20. Fang, T. Y., Zou, M., Simplaceanu, V., Ho, N. T., and Ho, C. (1999) Assessment of roles of surface histidyl residues in the molecular basis of the Bohr effect and of β143 histidine in the binding of 2,3-bisphosphoglycerate in human normal adult hemoglobin. *Biochemistry 38*, 13423–13432.
21. Arnone, A. (1972) X-ray-diffraction study of binding of 2,3-diphosphoglycerate to human deoxyhemoglobin. *Nature 237*, 146–149.
22. Arnone, A., and Perutz, M. F. (1974) Structure of inositol hexaphosphate-human deoxyhemoglobin complex. *Nature 249*, 34–36.
23. Marden, M. C., Kister, J., Bohn, B., and Poyart, C. (1988) T-state hemoglobin with 4 ligands bound. *Biochemistry 27*, 1659–1664.
24. Mozzarelli, A., Rivetti, C., Rossi, G. L., Eaton, W. A., and Henry, E. R. (1997) Allosteric effectors do not alter the oxygen affinity of hemoglobin crystals. *Protein Sci. 6*, 484–489.
25. Yonetani, T., Park, S., Tsuneshige, A., Imai, K., and Kanaori, K. (2002) Global allostery model of hemoglobin—Modulation of O_2 affinity, cooperativity, and Bohr effect by heterotropic allosteric effectors. *J. Biol. Chem. 277*, 34508–34520.
26. Nagatomo, S., Nagai, M., Mizutani, Y., Yonetani, T., and Kitagawa, T. (2005) Quaternary structures of intermediately ligated human hemoglobin A and influences from strong allosteric effectors: Resonance Raman investigation. *Biophys. J. 89*, 1203–1213.
27. Laberge, M., and Yonetani, T. (2008) Molecular dynamics simulations of hemoglobin A in different states and bound to DPG: Effector-linked perturbation of tertiary conformations and HbA concerted dynamics. *Biophys. J. 94*, 2737–2751.
28. Bunn, H. F., and Forget, B. G., Eds. (1986) Hemoglobin: molecular, genetic and clinical aspects, W. B. Saunders, Philadelphia, PA.
29. Reed, C. S., Hampson, R., Gordon, S., Jones, R. T., Novy, M. J., Brimhall, B., Edwards, M. J., and Koler, R. D. (1968) Erythrocytosis secondary to increased oxygen affinity of a mutant hemoglobin hemoglobin Kempsey. *Blood 31*, 623–632.
30. Puius, Y. A., Zou, M., Ho, N. T., Ho, C., and Almo, S. C. (1998) Novel water-mediated hydrogen bonds as the structural basis for the low oxygen affinity of the blood substitute candidate rHb(α96Val → Trp). *Biochemistry 37*, 9258–9265.
31. Russu, I. M., Ho, N. T., and Ho, C. (1987) A proton nuclear Overhauser effect investigation of the subunit interfaces in human normal adult hemoglobin. *Biochim. Biophys. Acta 914*, 40–48.
32. Chang, C. K., Simplaceanu, V., and Ho, C. (2002) Effects of amino acid substitutions at β131 on the structure and properties of hemoglobin: Evidence for communication between $\alpha_1\beta_1$- and $\alpha_1\beta_2$-subunit interfaces. *Biochemistry 41*, 5644–5655.
33. Maillett, D. H., Simplaceanu, V., Shen, T. J., Ho, N. T., Olson, J. S., and Ho, C. (2008) Interfacial and distal-heme pocket mutations exhibit additive effects on the structure and function of hemoglobin. *Biochemistry 47*, 10551–10563.
34. Lindstrom, T. R., and Ho, C. (1972) Functional nonequivalence of alpha and beta hemes in human adult hemoglobin. *Proc. Natl. Acad. Sci. U.S.A. 69*, 1707–1710.
35. Viggiano, G., and Ho, C. (1979) Proton nuclear magnetic resonance investigation of structural-changes associated with cooperative oxygenation of human adult hemoglobin. *Proc. Natl. Acad. Sci. U.S.A. 76*, 3673–3677.
36. Song, X. J., Simplaceanu, V., Ho, N. T., and Ho, C. (2008) Effector-induced structural fluctuation, regulates the ligand affinity of an allosteric protein: Binding of inositol hexaphosphate has distinct

dynamic consequences for the T and R states of hemoglobin. *Biochemistry 47*, 4907–4915.
37. Gong, Q. G., Simplaceanu, V., Lukin, J. A., Giovannelli, J. L., Ho, N. T., and Ho, C. (2006) Quaternary structure of carbonmonoxyhemoglobins in solution: Structural changes induced by the allosteric effector inositol hexaphosphate. *Biochemistry 45*, 5140–5148.
38. Yuan, Y., Simplaceanu, V., Lukin, J. A., and Ho, C. (2002) NMR investigation of the dynamics of tryptophan side-chains in hemoglobins. *J. Mol. Biol. 321*, 863–878.
39. Sahu, S. C., Simplaceanu, V., Gong, Q., Ho, N. T., Tian, F., Prestegard, J. H., and Ho, C. (2007) Insights into the solution structure of human deoxyhemoglobin in the absence and presence of an allosteric effector. *Biochemistry 46*, 9973–9980.
40. Fung, L. W. M., and Ho, C. (1975) Proton nuclear magnetic resonance study of quaternary structure of human hemoglobins in water. *Biochemistry 14*, 2526–2535.
41. Perutz, M. F. (1970) Stereochemistry of cooperative effects in haemoglobin. *Nature 228*, 726–739.
42. Silva, M. M., Rogers, P. H., and Arnone, A. (1992) A 3rd quaternary structure of human hemoglobin-A at 1.7Å resolution. *J. Biol. Chem. 267*, 17248–17256.
43. Smith, F. R., and Simmons, K. C. (1994) Cyanomet human hemoglobin crystallized under physiological conditions exhibits the Y-quaternary structure. *Proteins: Struct., Funct., Genet. 18*, 295–300.
44. Safo, M. K., and Abraham, D. J. (2005) The enigma of the liganded hemoglobin end state: A novel quaternary structure of human carbonmonoxy hemoglobin. *Biochemistry 44*, 8347–8359.
45. Tame, J. R. H., and Vallone, B. (2000) The structures of deoxy human haemoglobin and the mutant Hb Tyrα42His at 120 K. *Acta Crystallogr., Sect. D: Biol. Crystallogr. 56*, 805–811.
46. Fermi, G., Perutz, M. F., Shaanan, B., and Fourme, R. (1984) The crystal structure of human deoxyhaemoglobin at 1.74 Å resolution. *J. Mol. Biol. 175*, 159–174.
47. Liddington, R., Derewenda, Z., Dodson, E., Hubbard, R., and Dodson, G. (1992) High resolution crystal structures and comparisons of T-state deoxyhaemoglobin and two liganded T-State haemoglobins: T(α-oxy)haemoglobin and T(met)haemoglobin. *J. Mol. Biol. 228*, 551–579.
48. Seixas, F. A. V., de Azevedo, W. F., and Colombo, M. F. (1999) Crystallization and X-ray diffraction data analysis of human deoxyhaemoglobin A_0 fully stripped of any anions. *Acta Crystallogr., Sect. D: Biol. Crystallogr. 55*, 1914–1916.
49. Kavanaugh, J. S., Rogers, P. H., and Arnone, A. (2005) Crystallographic evidence for a new ensemble of ligand-induced allosteric transitions in hemoglobin: The T-to-T-high quaternary transitions. *Biochemistry 44*, 6101–6121.
50. Kavanaugh, J. S., Moopenn, W. F., and Arnone, A. (1993) Accommodation of insertions in helices—The mutation in hemoglobin Catonsville (Pro 37α-Glu-Thr 38α) generates a $3_{10} \rightarrow \alpha$ bulge. *Biochemistry 32*, 2509–2513.
51. DeLano, W. L. (2002) The PyMOL molecular graphics system (http://www.pymol.org), DeLano Scientific, Palo Alto, CA.
52. Baldwin, J., and Chothia, C. (1979) Haemoglobin: The structural changes related to ligand binding and its allosteric mechanism. *J. Mol. Biol. 129*, 175–200.
53. Manning, L. R., Russell, J. E., Padovan, J. C., Chait, B. T., Popowicz, A., Manning, R. S., and Manning, J. M. (2007) Human embryonic, fetal, and adult hemoglobins have different subunit interface strengths. Correlation with lifespan in the red cell. *Protein Sci. 16*, 1641–1658.
54. Manning, L. R., Russell, J. E., Popowicz, A. M., Manning, R. S., Padovan, J. C., and Manning, J. M. (2009) Energetic differences at the subunit interfaces of normal human hemoglobins correlate with their developmental profile. *Biochemistry 48*, 7568–7574.
55. Valdes, R., and Ackers, G. K. (1977) Thermodynamic studies on subunit assembly in human hemoglobin—Self-association of oxygenated chains (α^{SH} and β^{SH})—Determination of stoichiometries and equilibrium-constants as a function of temperature. *J. Biol. Chem. 252*, 74–81.
56. Song, X. J., Yuan, Y., Simplaceanu, V., Sahu, S. C., Ho, N. T., and Ho, C. (2007) A comparative NMR study of the polypeptide backbone dynamics of hemoglobin in the deoxy and carbonmonoxy forms. *Biochemistry 46*, 6795–6803.
57. Lukin, J. A., Kontaxis, G., Simplaceanu, V., Yuan, Y., Bax, A., and Ho, C. (2003) Quaternary structure of hemoglobin in solution. *Proc. Natl. Acad. Sci. U.S.A. 100*, 517–520.